2004

Modeling and Testing of an Automobile AC Scroll Compressor, Part I: Model Development

Feng Shou Yi
Nanjing Aotecar Refrigeration Compressor Co.

Eckhard A. Groll
Purdue University

James A. Braun
Purdue University

MODELING AND TESTING OF AN AUTOMOBILE AC SCROLL COMPRESSOR, PART I: MODEL DEVELOPMENT

Fengshou Yi[(1)] Eckhard A. Groll[(2)] James E. Braun[(2)]

[(1)]Nanjing Aotecar Refrigeration Compressor Co., Ltd,
No.103 Daming Road, Nanjing, Jiangsu, PR. China, Zip 210012
Tel: 86-25-52193204; Fax 86-25-52600072; E-mail: y1fs@hotmail.com

[(2)]Purdue University, Ray W. Herrick Laboratories,
140 S. Intramural Drive West Lafayette, IN 47907, USA
Tel: 765-496-2201; Fax: 765-494-0787; E-mail: groll@ecn.purdue.edu

ABSTRACT

This paper presents the details of an overall simulation model that predicts the performance of an automobile air conditioning scroll compressor. Using the overall model, the compressor performance and discharge temperature can be predicted at specific operating conditions. The model will be used in the future to optimize the design of automobile air conditioning scroll compressors. The model was developed based on an investigation of the geometric characteristic of an existing compressor, the modeling of the compression process, and an efficiency analysis. The pre-compression at the end of the suction process and re-compression at the discharge angle are taken into account in the process model. Tangential leakage and radial leakage during the compression process are investigated within the efficiency analysis. The influence of superheat and heat transfer during the compression process on performance are also taken into account within the efficiency analysis.

1. INTRODUCTION

As environmental protection and energy conservation become more important, the need for high efficiency compressors increases. Scroll compressors are high efficiency compressors that were developed in the past 20 years. In the automobile air conditioning field, high performance and reliable compressors are required as a result of tense market competition. Scroll compressors meet these requirements and were developed for this application in the past decade. Many research studies involving scroll compressors modeling and experiments were conducted in the past years. However, most of these research studies focused on scroll compressors for residential and light commercial air conditioning applications. Only few research studies have been conducted on automotive AC scroll compressors. This paper and the companion Part II paper present the model development, testing and model validation of an automotive AC scroll compressor. This paper describes the simulation model development.

2. GEOMETRY CHARACTERISTIC

2.1 The definition of various compressor chambers

When the orbiting and fixed scrolls conjugate, several chambers are formed within the scrolls. For ease of analysis, these chambers are marked by numbers, as shown in Figure 1. The chamber formed by the fixed inner scroll tail and the orbiting outer scroll is chamber 1; the chamber formed by the orbiting inner scroll tail and the fixed outer scroll is chamber 2; chamber 3 is the chamber developed from chamber 1; chamber 4 is the chamber developed from chamber 2; the innermost chamber is chamber 7. When chamber 3 and chamber 4 are open to chamber 7 at some orbiting angle, there is gas exchange among them. If the pressures in chamber 3 and chamber 7 have equalized, the control volume is labeled as chamber 8. If the pressures of chamber 4 and chamber 7 have equalized, the control volume is labeled as chamber 9. In the case that the pressures of chamber 3, chamber 4, and chamber 7 have equalized, the entire control volume will be treated as chamber 10. If the pressures of chamber 3, chamber 4, and chamber 7 have not equalized when chamber 1 has closed and is to reopen, a new chamber 1 is formed and the old chamber 1 becomes chamber 3 and the old chamber 3 becomes chamber 5. Similarly, if the pressure of the innermost chamber has not equalized to its neighbor chambers when chamber 2 has closed and is to reopen, the old

chamber 2 becomes chamber 4, and the old chamber 4 becomes chamber 6. A similar approach is described by Chen *et al.* (2000). Therefore, in an entire revolution, thirteen cases of different chambers coexisting are possible as listed in Table 1. Note that the orbiting angle is zero at the moment when the end of the fixed scroll is closed and just to be re-opened.

Table 1: Definition of cases of the scroll compressor chamber configurations

Case	Scroll compressor chamber										Orbiting angle θ	Comment
	1	2	3	4	5	6	7	8	9	10		
1	*	*	*		*	*	*				$0< \theta \leq \phi_{oe}$	P_7 is different with P_5 and P_6
2	*	*	*		*				*			P_7 and P_6 become equal, and not equal to P_5
3	*	*	*			*		*				P_7 and P_5 become equal, and not equal to P_6
4	*	*	*							*		P_7, P_5 and P_6 become equal
5	*	*	*		*	*	*				$\phi_{oe} < \theta \leq \phi_{56end}$	P_7 is different with P_5 and P_6
6	*	*	*	*	*				*			P_7 and P_6 become equal, and not equal to P_5
7	*	*	*	*		*		*				P_7 and P_5 become equal, and not equal to P_6
8	*	*	*	*						*		P_7, P_5 and P_6 become equal,
9	*	*	*	*						*	$\phi_{56end} < \theta \leq \phi_d$	Chamber 5 and 6 end, chamber 7 starts from maximum volume
10	*	*	*	*			*				$\phi_d < \theta \leq 2\pi$	P_7 is different with P_3 and P_4
11	*	*	*						*			P_7 and P_4 become equal, and are treated as P_9
12	*	*		*				*				P_7 and P_3 become equal, and are treated as P_8
13	*	*								*		P_7, P and P_4 become equal

Explanation: 1. '*' means the chamber exists at this case.
2. P_7 means the pressure of chamber 7, P_3 means the pressure of chamber 3, etc.

2.2 The calculation of various chamber volumes

The volume of each chamber is the product of its enclosed area and the height of the wrap. The enclosed area for chamber 1 is the area enclosed by the fixed inner scroll from the conjugating angle ϕ_k to the end involute angle ϕ_e, and the orbiting outer scroll from $\phi_k - \pi$ to $\phi_e - \pi$, and the segment, which is from the fixed scroll end and the tangent of the basic circle. The enclosed area for chamber 2 is the area enclosed by the orbiting inner scroll from the conjugating angle ϕ_k to ϕ_{oe}, and the fixed outer scroll from $\phi_k - \pi$ to $\phi_{oe} - \pi$, and the segment, which is from the orbiting scroll end and the tangent of the basic circle. The enclosed area for chamber 3 is the area enclosed by the fixed inner scroll from ϕ_k to $\phi_k - 2\pi$, and the orbiting outer scroll from $\phi_k - \pi$ to $\phi_k - 3\pi$. The enclosed area for chamber 4 is equal to that of chamber 3. The enclosed areas for chambers 5 and 6 are similar to chambers 3 and 4, and can be obtained by subtracting 2π from the respective involute angles. The inner most area is enclosed by lines, arcs and involutes. The enclosed area can be integrated and only has a numerical solution.

The calculated volumes of each chamber are shown in Figure 2. Chambers 1 and 2 are suction chambers. It can be seen that the volume of chamber 1 increases from a zero value at 0^0 to a maximum value of 45 cm^3 at 311^0, and then gradually decreases to 43 cm^3 at 360^0. Since the orbiting scroll is a little shorter than the fixed scroll, it closes later. Therefore, the volume of chamber 2 increases from a zero value at 11^0 to a maximum value of 44.5 cm^3 at 320^0, and then gradually decreases to 42.6 cm^3 at 371^0. Chambers 3 and 4 are compression chambers. It can be seen that their volume are equal to each other, and decrease linearly from the end of the suction chambers to 720^0. After 720^0, they transfer into chambers 5 and 6, respectively, and continue to decrease until 750^0. At 750^0, they open to the inner most chamber (chamber 7), and at that time the volume of chamber 7 reaches its maximum value. The volume of

chamber 7 decreases gradually from 750^0, until new chambers 5 and 6 re-open to chamber 7 after another revolution.

3. COMPRESSION PROCESS MODEL

The compression process model is based on the first law of thermodynamics for an open control volume, mass balances, and property equations.

3.1 Differential equations governing the compression process

The first law of thermodynamics for an open control volume can be written as follow (Chen *et al.,* 2000):

$$\frac{dT}{d\theta}=\frac{1}{mC_v}\left\{-T\left(\frac{\partial P}{\partial T}\right)_v\left[\frac{dV}{d\theta}-\frac{v}{\omega}\left(\dot{m}_{in}-\dot{m}_{out}\right)\right]-\sum\frac{\dot{m}_{in}}{\omega}(h-h_{in})+\frac{\dot{Q}}{\omega}\right\} \tag{1}$$

and the mass balance equation is written:

$$\frac{dm}{dt}=\sum\frac{\dot{m}_{in}}{\omega}-\sum\frac{\dot{m}_{out}}{\omega} \tag{2}$$

Equation (1) represents a first-order differential equation with the independent variables of temperature T and mass m that needs to be integrated numerically. Together with the mass balance equation (2) and the equation of state for the refrigerant, equation (1) provides a relationship to calculate the thermodynamic properties in each compression chamber as a function of orbiting angle. In order to evaluate equation (1), models that predict the mass flow rate into and out of each chamber as well as heat transfer rate are required. Also, expressions for the change of pressure with respect to temperature at constant specific volume, and for enthalpies h and h_{in} are required.

3.2 Real gas property

The investigated compressor uses R-134a as its refrigerant. Tillner-Roth and Baehr (1994) presented a fundamental equation of state based on the Helmholz free energy of R-134a that is valid for temperatures between 170 K and 455 K and pressure up to 70 MPa. The property relationship is written into the computer code.

$$P=p(\rho,T) \tag{3}$$

$$\frac{\partial P}{\partial T}=f(\rho,T) \tag{4}$$

3.3 Suction process

For the investigated compressor, the refrigerant is sucked into a suction room through the suction port. The scrolls are immersed in the refrigerant in the suction room. When the conjugating scrolls form a pair of crescent chambers that open to the suction room, the refrigerant in the suction room fills into the crescent chambers. The crescent chambers are named suction chambers. With the suction chambers enlarging due to the orbiting angle proceeding, more and more gas is trapped into them. After the crescent chamber reaches its maximum volume the gas in them begins to be compressed since the volume starts to reduce. The chamber port formed by the scrolls is still opening at that time. Therefore some gas in the suction chambers goes out to suction room through the chamber ports. The mass flow rate through the chamber port can be calculated by using the flow equation for isentropic flow of compressible ideal gas. A flow factor ψ is employed to correct the calculation.

$$\dot{m}=\psi A_s\sqrt{2P_h\rho_h\frac{k}{k-1}\left[\left(\frac{P_l}{P_h}\right)^{\frac{2}{k}}-\left(\frac{P_l}{P_h}\right)^{\frac{k+1}{k}}\right]} \tag{5}$$

When the pressure ratio is greater than the critical ratio, the critical pressure ratio is taken.

$$\left(\frac{P_l}{P_h}\right)_{cri}=\left(\frac{2}{k+1}\right)^{\frac{k}{k-1}} \tag{6}$$

The pre-compression process goes on until the chamber ports close. The pre-compression process increases the compressor's volumetric efficiency.

3.4 Compression process

The compression process starts when the suction chamber port closes. The pressure in the compression chamber increases with the orbiting angle increasing. If the leakage and heat transfer are known, the temperature of the refrigerant during the compression process can be calculated by (1). The density of the refrigerant in the chamber can be calculated by its ratio of mass to chamber volume. The pressure of the refrigerant during the compression process can be calculated by the real gas property equation of state (3). Since the leakage and heat transfer are related to the pressure and temperature in the compression process, an iteration method is employed to calculate the properties. When the difference between the assumed value and the calculated result is small enough, the calculation result is treated reasonable.

The compression process is supposed to end when the compression chambers (chambers 3 and 4) open up to chamber 7. However, for most operating conditions, the investigated compressor operates at pressure ratios that are higher than the built-in pressure ratio. Therefore, the gas in chamber 7 flows back to chambers 3 and 4 when chambers 3 and 4 open up to chamber 7. Additional compression occurs with increasing orbiting angle and the discharge process starts when the compression pressure is greater than the line backpressure.

3.5 Discharge process

When the pressure in chamber 7 is greater than the backpressure, the refrigerant opens the check valve and is discharged through a chamber discharge port. The open extent of the check valve is related to the pressure difference between the inner pressure and outer pressure. Before the valve touches the valve stop, the valve motion can be described by equation (7):

$$y = \frac{(p - p_d)\pi \frac{d^2}{4} t^2}{2m_{valve} + \frac{EBH^3}{4l^3}} \tag{7}$$

The maximum distance that the valve can travel is determined by the valve stop.

$$y \le y_{stop} \tag{8}$$

The flow through the discharge port is modeled as flow through an orifice by using equation (9)

$$\dot{m} = y\pi d\rho\sqrt{\frac{2\Delta p}{\rho}} \tag{9}$$

4. EFFICIENCY ANALYSIS

Leakage, heat transfer, and mechanical friction are the primary factors that influence a compressor's efficiency. For the investigated scroll compressor, the shaft is supported by ball bearings, and the mechanical friction is small. Therefore, only the influences of leakage and heat transfer are discussed in this paper even though all of them are taken into account in the simulation model.

4.1 Leakage

The leakage of the scroll compressor has been presented in detail in another paper (Yi et al., 2003). Thus, only a brief review is given here. A nozzle flow model is employed to compute the leakage flow between the chambers. The formula is presented in Equation (5). When the pressure ratio is greater than the critical pressure ratio, the critical ratio is taken as shown in Equation (6). Figure 3 is a schematic of the scroll compressor's seal system. There is a groove in the tip of scroll wrap. A seal element is inserted in the groove to prevent leaking. A steel plate covers the scroll bottom to prevent wear. The clearance C is the clearance between the scroll wrap and the steel plate groove and can be expressed as δ_c. The clearance B is the clearance between the wraps tip and the steel surface and can be expressed as δ_b. The clearance A is the clearance between the seal element and the scroll wrap groove and

can be expressed as δ_a. The flank clearance δ_f is the clearance between the scroll wraps. The tip clearance δ_{tip} is the clearance between the seal element and the steel plate. The leakages through δ_a, δ_b, δ_c and δ_f flow out tangentially. The length of each leakage line is equal to the height of the scroll. Thus, the total leakage area for the tangential leakage is given by Equation (10).

$$A_t = \delta_f h + \frac{1}{2}(t - w_{seal})\delta_b + (w_{groove} - w_{seal})h_{groove} + (w_{steel} - t)t_{steel} \tag{10}$$

The leakage area for the radial leakage is given Equation (11)

$$A_r(\phi) = \delta_r \int_{\phi_s}^{\phi_e} r_b \phi^2 d\phi \tag{11}$$

where $\delta_r = \delta_b$ when $\phi_{eseal} \le \phi < \phi_e$ or $\phi < \phi_{sseal}$

or $\delta_r = \delta_{tip}$ when $\phi_{sseal} \le \phi < \phi_{eseal}$

4.2 Heat transfer

When the refrigerant passes through the compressor chambers, it is heated by the shell and the scrolls. The heat transfer changes the refrigerant's temperature, as well as its density. The mass flow rate is reduced if the density of the suction gas is decreased. In addition, heat transfer in the compression process may increase or decrease the compression work. Therefore, heat transfer is another important factor that influences the compressor's performance. In order to simplify the investigation on heat transfer, the following assumptions were made:

- The properties of the refrigerant and oil mixture, except the specific heat, are the same as the ones of the pure refrigerant since the percentage of the oil is less than 4%. The specific heat of the mixture is computed according to their mass percentages and specific heats, respectively.
- The heat transfer between the refrigerant and the oil is instantaneous with no heat resistance. Thus, the mixture of refrigerant and oil in one chamber are at the same temperature.

A schematic of a section of the compressor is shown in Figure 4. The refrigerant is sucked from the suction port, passes through the suction channel and the chambers, and then is discharged through the check valve into the discharge volume. From there, it leaves the compressor through the discharge port. $\dot{Q}_{sch}$ is the heat transfer rate that transfers heat from the suction channel to the refrigerant when the refrigerant passes through the suction channel, as shown in Figure 5. $\dot{Q}_{sc}$ is the heat transfer rate that transfers heat from the suction chamber walls to the refrigerant when the refrigerant passes through the suction chambers. $\dot{Q}_{cc}$ is the heat transfer rate that transfers heat from the compression chamber walls to the refrigerant when the refrigerant passes through the compression chambers. $\dot{Q}_{dc}$ is the heat transfer rate that transfers heat from the discharge chamber walls to the refrigerant when the refrigerant passes through the discharge chamber. $\dot{Q}_{br}$ is the heat transfer rate that transfers heat from the discharge volume walls to the refrigerant when the refrigerant passes through the discharge volume.

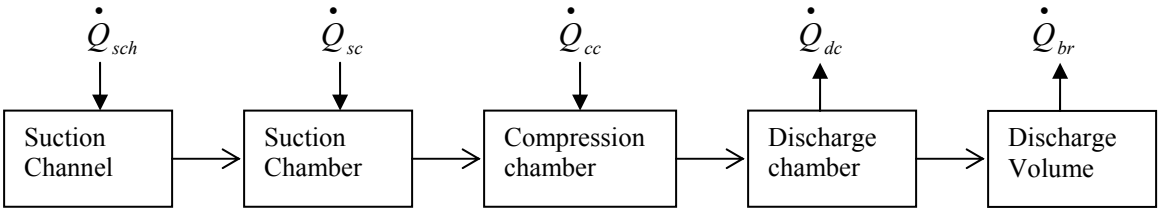

The suction channel heat transfer rate, $\dot{Q}_{sch}$, is calculated by Equation (12).

$$\dot{Q}_{sch} = \frac{T_{fshell} - T_s}{R_{s-shell}} \tag{12}$$

The heat transfer resistant $R_{s-shell}$ is calculated using a model for pipe flow and revised by a coefficient that comes from the experimental data. The suction chamber, compression chamber and discharge chamber heat transfer rates, $\dot{Q}_{sc}$, $\dot{Q}_{cc}$, and $\dot{Q}_{dc}$, are calculated by using a spiral heat exchanger model (Chen, 2000). The heat transfer coefficients are approximated with a correlation for a spiral tube exchanger as shown in Equation (13).

$$h_c = 0.023 \frac{k}{D_h} \mathrm{Re}^{0.8}\, \mathrm{Pr}^4 (1.0 + 1.77 \frac{D_h}{r_{aver}}) \tag{13}$$

where
$$D_h = \frac{4V}{A} \tag{14}$$

and
$$r_{aver} = r_b \left[\frac{(\phi_k - 0.5\pi + (\phi_{k-1} - 0.5\pi)}{2} \right] \tag{15}$$

Where ϕ_k and ϕ_{k-1} are the bounding involute angles of a respective chamber.

The temperature distribution of the scroll is non-uniform. Based on experimental results, the scroll temperature distribution can be approximated by a two-order polynomial equation as a function of the involute angle as shown in Equation (16).

$$T(\phi) = c_1 + c_2\phi + c_3\phi^2 \tag{16}$$

The heat flow rate from the scroll walls/plates to the refrigerant in any chamber can then be calculated by an integral method according to equation (17).

$$\dot{Q} = h_c \int_A [T(\phi) - T(k, j)] dA \tag{17}$$

Where $T(k, j)$ is the refrigerant temperature in kth chamber at the orbiting angle θ_j. The heat transfer rate from the scroll wraps between involute angles ϕ_k and $\phi_k - 2\pi$ is determined by Equation (18).

$$\dot{Q}_w = h r_b h_c \int_{\phi_k - 2\pi}^{\phi_k} [T(\phi) - T(k, j)](\phi - \phi_0) d\phi \tag{18}$$

Where $\phi_0 = \phi_{ii}$ for the inner side wall, and $\phi_0 = \phi_{io}$ for the outer side wall. Assuming that the temperature of the plate is equal to the average temperature of the two enclosing wraps, the heat transfer rate from the plate is determined by Equation (19).

$$\dot{Q}_p = h_c \int_{\phi_s}^{\phi_e} [T(\phi) - T(k, j)] \frac{1}{2} r_b^2 \left[(\phi - \phi_{ii})^2 - (\phi - \pi - \phi_{io})^2 \right] d\phi \tag{19}$$

Where ϕ_s is the starting involute angle for the chamber, and ϕ_e is the end involute angle for the chamber. Thus, for any chamber, the total heat transfer rate is equal to the heat transfer rates from the two plates and the two wraps. The total heat transfer rate is calculated by Equation (20).

$$\dot{Q} = 2\dot{Q}_p(\phi) + \dot{Q}_w(\phi) + \dot{Q}_w(\phi - \pi) \tag{20}$$

Where $\dot{Q}_{br}$ is the sum of $\dot{Q}_{sch}$ and $\dot{Q}_{release}$. $\dot{Q}_{release}$ can be calculated using a free convection model for a cylinder and plane.

All of the heat transfer rates are employed in Equation (1) to calculate the temperature of the refrigerant in each chamber at any orbiting angle. The temperature influences the mass flow rate and the compression power of the compressor. Therefore, heat transfer influences the compressor efficiency indirectly.

5. CONCLUSION

This paper presents a simulation model of an automotive open-drive scroll compressor. The geometry of the compressor was investigated. The properties of the refrigerant throughout the compression process are calculated by using the first law of thermodynamics for an open control volume. All processes that the refrigerant experiences from the inlet to the outlet of the compressor are taken into account including suction pre-compression, leakages among the chambers, and heat transfer during the compression process.

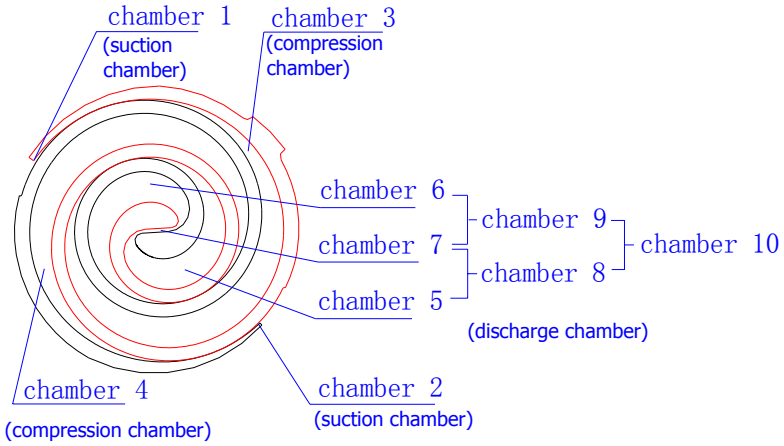

Figure 1: The definition of chambers for the scroll compressor

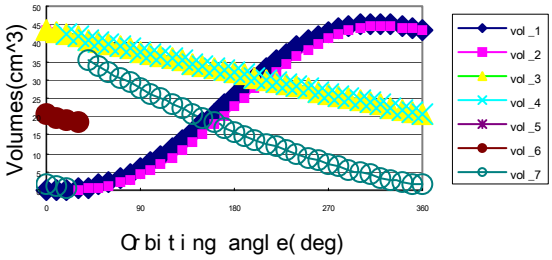

Figure 2: The volumes of each chamber for the scroll compressor

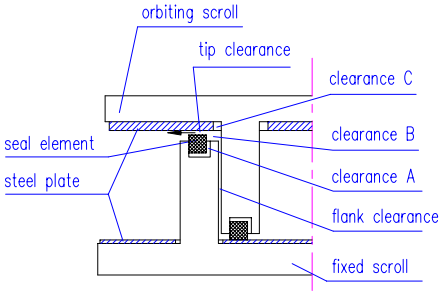

Figure 3: Clearances in the scroll compressor

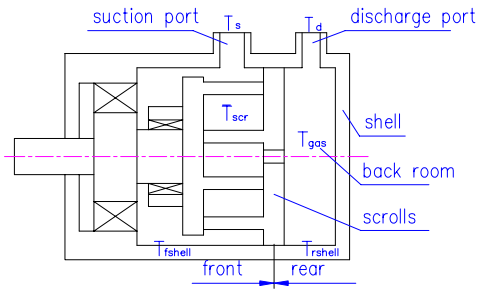

Figure 4: Schematic of the scroll compressor

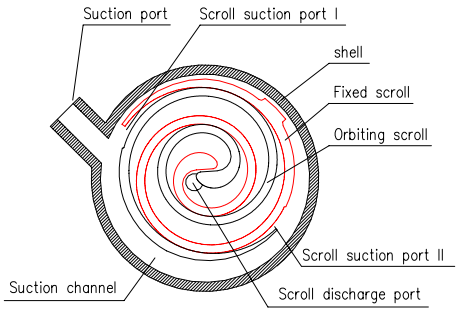

Figure 5: A section of the suction channel

NOMENCLATURE

A_s area
B width of discharge valve
c constant coefficient
Cv specific heat at constant specific volume
d diameter of chamber discharge port
E material elastic coefficient for the check valve
h height of the involutes wraps
h specific enthalpy
H thickness of discharge valve
h_{in} specific enthalpy of inlet
k specific ratio
l length of discharge valve
m mass
$\dot{m}$ mass flow rate
m_{valve} mass of valve
$\dot{m}_{in}$ mass flow rate into control volume
$\dot{m}_{out}$ mass flow rate out control volume
P pressure
P_d discharge pressure
P_h pressure of high pressure side
P_l pressure of low pressure side
$\dot{Q}$ heat transfer rate
$\dot{Q}_P$ heat transfer between scroll plates and refrigerant
$\dot{Q}_w$ heat transfer between scroll wraps and refrigerant
$\dot{Q}_{release}$ Heat transfer from shell to ambience
R_{aver} average radius of curved chamber
r_b radius of basic circle
r_o orbiting radius
T temperature
t time
t width of scroll wrap
T_{fshell} average temperature of front shell
T_s average suction temperature
t_{steel} thickness of steel plate
V control volume
W width
y moving distance of the discharge vale
y_{stop} maximum moving distance

ϕ involute angle of an involute
ϕ_{ii}: initial angle of inner involute
ϕ_{io} initial angle of outer involute
ϕ_k conjugating involute angle
ϕ_e end involute angle of fixed scroll
ϕ_{eseal} end involute angle of seal element
ϕ_{oe} end involute angle of orbiting scroll
ϕ_{sseal} start involute angle of seal element
ν specific volume
θ orbiting angle
θ_d discharge angle
ρ density
ω angular speed of compressor shaft

REFERENCES

Chen, Y., Halm, N.P., Groll, E.A., and J.E. Braun, "Mathematical Modeling of Scroll Compressors Part I: Compression Process Modeling," *Int'l J. Refrig.*, Vol. 25, No. 7, 2002, pp. 731-750.

Tillner-Roth, R., and H.D. Baehr, "An International Standard Formulation for Thermodynamic Properties of 1,1,1,2-Tetrafluoroethane (HFC-134a) for Temperature From 170 K to 455K and Pressure up to 70 MPa," *J. Phys.Chem. Ref. Data*, Vol. 23, No.5, 1994, pp. 657-675.

Yi, F., Groll, E.A., and J.E. Braun, "A Study on the Leakage of an Automobile Scroll Compressor, *Proceedings of the 4th International Conference on Compressors and Refrigeration*, Xi'an, China, 2003, pp. 15-24.

ACKNOWLEDGEMENT

The authors appreciate the financial support of Nanjing Aotecar Refrigeration Compressor Company to conduct the study and the permission to publish the two-part papers.